Azimuthal phase speeds of field line resonances driven by Kelvin-Helmholtz unstable waveguide modes

Katharine J. Mills and Andrew N. Wright

Mathematical Institute, University of St. Andrews, St. Andrews, Fife, Scotland

Abstract. A model for the coupling of Kelvin-Helmholtz unstable fast cavity modes to field line resonances (FLRs) is presented. We consider a bounded, nonuniform magnetospheric flank separated from a semi-infinite, field-free, flowing magnetosheath by an infinitely thin magnetopause. Fast cavity modes may become unstable for sufficiently high flow speeds, and we find that for any flow speed there is a common phase speed at which all the harmonics have their maximum growth rate. The common phase speed is less dependent on the equilibrium structure within the magnetosphere than on the local structure of density ratio and relative velocity jump at the magnetopause. We perform a local analysis of the reflection and transmission of modes at the magnetopause. By requiring the spontaneous radiation of modes from the magnetopause, we may predict a phase speed at which we would expect the maximum growth rate to occur for any set of parameters. These predicted phase speeds are found to be in agreement with both those found by our model and observations of FLRs that are observed simultaneously at different latitudes.

1. Introduction

Ultralow frequency (ULF) waves are observed almost continuously on the flanks of the magnetosphere [e.g., *Engebretson et al.*, 1998]. It was first suggested by *Dungey* [1955] that these pulsations were standing toroidal Alfvén modes on the dipolar field lines of the Earth. *Southwood* [1974] suggested that surface modes driven by the Kelvin-Helmholtz instability at the magnetopause could couple to the Alfvén waves, feeding energy into these field line resonances (FLRs). However, the magnetosheath velocities required to drive the FLRs by this mechanism were found to be much higher than those observed [*Hughes*, 1994], and the frequencies of the FLRs driven in this way do not explain the low frequencies observed [*Walker et al.*, 1992].

Kivelson and Southwood [1985] showed that in a nonuniform magnetosphere, a turning point exists within the magnetosphere beyond which only an evanescent tail of a cavity mode may propagate. The Alfvén resonance is then thought to be driven by this evanescent tail. The frequencies of these oscillations have been predicted through various models [e.g. *Kivelson and Southwood*, 1986] using the eigenfrequencies of the magnetospheric cavity to predict the frequencies of the FLRs. *Wright* [1994] and *Rickard and Wright* [1994, 1995] showed how the waveguide cutoff frequen-

cies could also match FLR frequencies. However, recent observations by *Ziesolleck and McDiarmid* [1994] showed that FLRs observed simultaneously at different latitudes on the flanks of the magnetosphere can have the same azimuthal phase speed, and it is this phenomenon that we aim to explain. *Wright and Rickard* [1995] have already noted that such observations are consistent with resonances driven by a running pulse on the magnetopause rather than by a stationary pulse. In this paper we identify a new mechanism associated with Kelvin-Helmholtz excited waveguide modes. We show that the azimuthal phase speeds of the waveguide mode and the FLR it can excite are the same.

We employ the theory of overreflection of waves [*McKenzie*, 1970]. *McKenzie* [1970] modeled an infinite, uniform magnetosphere and showed that for certain parameters a wave incident on the magnetopause from the magnetosphere will be amplified when reflected. Indeed, for certain phase speeds the transmission and reflection coefficients become infinite. This solution is better described in terms of the spontaneous radiation of modes from the magnetopause into the magnetosphere and magnetosheath. *Mann et al.* [1999] modeled a bounded uniform magnetosphere showing that oscillatory modes may also become unstable for realistic flow speeds and analyzing the reflection coefficient of these unstable modes, they showed that the maximum growth rate for each mode corresponded to a peak in the reflection coefficient. Mann et al. considered a uniform magnetosphere with perturbations only in the direction perpendicular to the magnetospheric magnetic field and so found no Alfvén resonances. *Mills et al.* [1999] con-

sidered a model similar to that of Mann et al.; however, they included a nonzero plasma beta and propagation of disturbances in all directions in the magnetopause plane. Once again, the uniform nature of the magnetosphere in that model prevented any Alfvén resonances. *Walker* [1998] gives a review of the theory of the excitation of the magnetospheric cavity, including a discussion showing that waves incident on the magnetopause from the magnetosheath may only be transmitted efficiently when their frequency matches that of one of the normal modes of the cavity.

We extend the models of *Mann et al.* [1999] and *Mills et al.* [1999] by using a generalized waveguide version of the box model of *Southwood* [1974]. It has a bounded nonuniform magnetosphere, with a free magnetopause boundary (i.e., the boundary may be disturbed, and we do not require the total reflection of modes back into the magnetosphere), and is similar to that studied by *Fujita et al.* [1996]. We find the fastest growing normal modes of this equilibrium subject to suitable boundary conditions. These modes may be interpreted as a negative energy wave in the magnetosheath which feeds energy into a magnetospheric cavity waveguide mode, which can in turn couple energy into Alfvén resonances within the magnetosphere. We show that the phase speed at maximum growth rate of the different harmonics is the same, and we show that this can be explained by the theory of overreflection developed by *McKenzie* [1970] [see also *Miles*, 1957; *Ribner*, 1957] and used by *Mann et al.* [1999]. We compare the phase speeds of the fastest growing Alfvén resonances (FLRs) with those predicted by the overreflection theory.

The structure of this paper is as follows: Section 2 outlines our model and the governing equations, and section 3 describes our numerical results. Section 4 describes the theory of wave overreflection and section 5 compares the numerical results to those obtained by the overreflection theory. Finally, section 6 summarizes our results.

2. Model and Equations

In this paper the flank equilibrium is modeled as a bounded, nonuniform magnetosphere adjoining a field-free, semi-infinite magnetosheath flowing with a constant velocity. This model is essentially that studied by *Fujita et al.* [1996]. Figure 1 shows a schematic view of our model. Throughout this paper we use variables normalized to the equilibrium sound speed, c_s, and density, ρ_2, in the magnetosheath and the width of the magnetospheric cavity, d. (Time is normalized by the quantity d/c_s, pressure is normalized by γP_2 and the magnetic fields are normalized by $\sqrt{\gamma P_2 \mu_o}$.) Thus the magnetopause is placed at $x = 1$. The field lines are taken to be finite in extent, which we have modeled by placing perfectly reflecting boundaries at $z = \pm 1$. The perfectly reflecting boundaries in z in the magnetosphere represent the fact that the field lines in this region have a finite length and are terminated in the ionosphere, which is an efficient reflector of Alfvén waves.

In order to study only the fast modes and their coupling to the Alfvén waves, we have assumed that $\beta = 0$ in the magnetosphere so that there is no plasma pressure. Thus, in order to vary the Alfvén speed v_a across the cavity, we must vary the equilibrium density, ρ_1. We have chosen a quadratic profile for the Alfvén speed, and the coefficients are fixed by choosing the ratio between the Alfvén speeds at the inner boundary and the magnetopause ($v_R = v_a(x = 0)/v_a(x = 1)$) and by taking the gradient of the profile to be zero at the magnetopause (so that close to the boundary the profile may be reasonably approximated as constant). Therefore our Alfvén speed profile is

$$v_a(x) = v_a(1)\left\{(v_R - 1)x^2 - 2(v_R - 1)x + v_R\right\}. \quad (1)$$

We find the value of $v_a(1)$ using total pressure balance at the magnetopause and the ratio of densities either side of the boundary so that

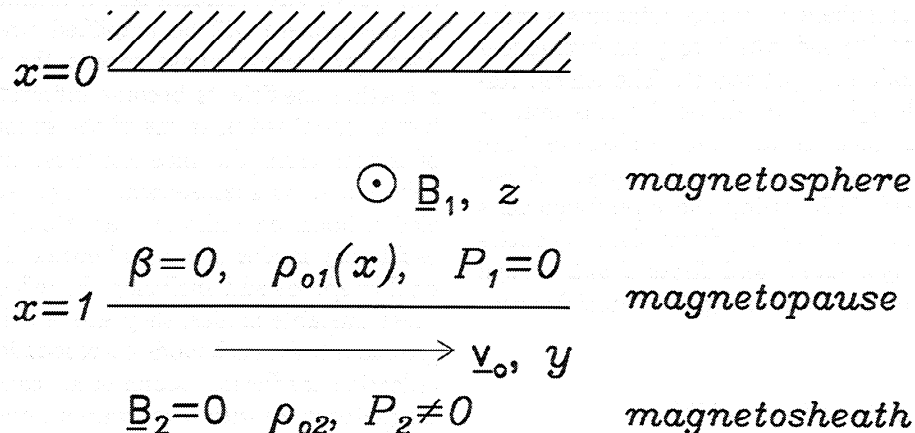$$v_a^2(1) = \frac{2}{\gamma}\frac{\rho_2}{\rho_1(1)}c_s^2. \quad (2)$$

$x=0$ ⧄⧄⧄⧄⧄⧄⧄⧄⧄⧄⧄⧄⧄

⊙ $\underline{B}_1$, z *magnetosphere*

$x=1$ $\beta=0$, $\rho_{o1}(x)$, $P_1=0$ *magnetopause*

⟶ $\underline{v}_o$, y

$\underline{B}_2=0$ ρ_{o2}, $P_2 \neq 0$ *magnetosheath*

Figure 1. A schematic representation of our bounded, nonuniform magnetosphere model.

In the magnetosheath the linearized ideal MHD equations may be combined to give a second-order ordinary differential equation (ODE) for the pressure perturbation,

$$\frac{d^2 p_2}{dx^2} + m_2^2 p_2 = 0. \tag{3}$$

Here m_2 is the x component of the wavenumber in the magnetosheath given by

$$m_2^2 = \frac{\omega'^2 - k^2 c_s^2}{c_s^2}. \tag{4}$$

Here, k is the total wavenumber tangential to the magnetopause given by $k = \sqrt{k_y^2 + k_z^2}$, where k_y and k_z are the wavenumbers in the y and z directions, respectively, and ω' is defined to be the Doppler-shifted frequency of the oscillations in the rest frame of the magnetosheath and is related to the frequency, ω, by

$$\omega' = \omega - k_y v_o. \tag{5}$$

Using the outgoing boundary condition to choose the sign of the root of m_2, we can find a solution in the magnetosheath to within a complex constant. The outgoing boundary condition requires that the x component of the group velocity of the waves in the magnetosheath is positive in the rest frame of the flowing plasma, which can be shown to be equivalent to requiring that

$$\mathrm{Re}\left(\omega'\right)\mathrm{Re}\left(m_2\right) + \mathrm{Im}\left(\omega'\right)\mathrm{Im}\left(m_2\right) > 0 \tag{6}$$

[see *Mann et al.*, 1999; *Mills et al.*, 1999]. The boundary condition, equation (6) can not be applied to real frequency modes as these are trapped in the magnetosphere and decay in the magnetosheath (i.e., they have no propagating character or group velocity in the magnetosheath). Such modes require m_2 to be imaginary and so can only occur when $\omega'^2 < k^2 c_{s2}^2$. The boundary condition we impose on these modes is that the perturbation vanishes at large x,

$$\mathrm{Im}\left(m_2\right) > 0. \tag{7}$$

In the magnetosphere we have combined the linearized ideal MHD equations to obtain two first-order differential equations for the perturbed total pressure p_T (which, since $\beta = 0$, is the magnetic pressure in the magnetosphere) and the x component of the perturbed velocity, u_x. The two ODEs are

$$\frac{dp_T}{dx} = i\rho_1\left(x\right)\left[\omega^2 - k_z^2 v_{a1}^2\left(x\right)\right]\frac{u_{x1}}{\omega}, \tag{8}$$

$$\frac{du_{x1}}{dx} = \frac{i\omega m_1^2\left(x\right)}{\rho_1\left(x\right)\left[\omega^2 - k_z^2 v_{a1}^2\left(x\right)\right]}p_T, \tag{9}$$

where m_1 is given from

$$m_1^2\left(x\right) = \frac{\omega^2 - k^2 v_a^2\left(x\right)}{v_a^2\left(x\right)} \tag{10}$$

and may be interpreted as the magnetosphere fast mode wavenumber in the x direction. Allowing a complex frequency, we actually have four equations for the real and imaginary parts of the velocity and pressure.

The inner boundary of the magnetosphere ($x = 0$) is assumed to be perfectly reflecting, and thus we take

$$u_x\left(x = 0\right) = 0, \tag{11}$$

which is equivalent to requiring that

$$\frac{dp_T}{dx}\left(x = 0\right) = 0. \tag{12}$$

Starting from this point, we integrate the four ODEs using a fourth-order Runge-Kutta method and match the solutions to those in the magnetosheath through the boundary conditions at the magnetopause, which are taken to be continuity of total pressure and displacement in the x direction, ξ_x,

$$p_T\left(x = 1\right) = p_2\left(x = 1\right), \tag{13}$$

$$\xi_{x1}\left(x = 1\right) = \frac{u_{x1}}{\omega}\left(x = 1\right) =$$
$$\frac{u_{x2}}{\omega - k_y v_o}\left(x = 1\right) = \xi_{x2}\left(x = 1\right). \tag{14}$$

Our dispersion relation is expressed as the following two equations, which are evaluated at $x = 1$,

$$\mathrm{Re}\left(\frac{p_T}{\xi_{x1}}\right) = \mathrm{Re}\left(\frac{p_2}{\xi_{x2}}\right), \tag{15}$$

$$\mathrm{Im}\left(\frac{p_T}{\xi_{x1}}\right) = \mathrm{Im}\left(\frac{p_2}{\xi_{x2}}\right). \tag{16}$$

Equations (15) and (16) are then solved using a two-dimensional Newton-Raphson method.

There is a singularity in the ODEs, equations (8) and (9), at

$$\omega^2 - k_z^2 v_a^2\left(x\right) = 0, \tag{17}$$

which for real ω occurs when

$$\omega = \pm k_z v_a\left(x\right). \tag{18}$$

The singularity is associated with an Alfvén resonance at the position x defined via equation (18) [see *Southwood*, 1974]. For real ω it is not possible to integrate along the real x axis as this contains a singularity, and so we cannot solve our dispersion relation numerically in this case. For complex $\omega = \omega_r + i\omega_i$, equation (17) becomes

$$\omega_r^2 - \omega_i^2 - k_z^2 v_a^2\left(x\right) + 2i\omega_r\omega_i = 0, \tag{19}$$

and the singularity is removed from the real x axis and moves into the complex x plane. Thus, for unstable modes, we may integrate across the magnetospheric cavity (i.e., along the real x axis), and solve our dispersion relation. As we are interested in studying the fastest growing modes in our system, the singular behavior for real ω poses no problems in our study. Note that the singularity (even at complex x) is actually a branch pole. Integration along the real x axis for modes that decay in time is not straightforward, since the branch cut will be encountered. With some care this case can be treated too [Zhu and Kivelson, 1988].

We define the resonant point, x_R, such that

$$v_a(x_R) = \frac{\omega_r}{k_z}, \qquad (20)$$

i.e., at the point at which a singularity would occur for real ω. We also define the turning point, x_t, to be the point at which the nature of the mode in the magnetosphere changes from oscillatory to evanescent. For real ω this point is defined by

$$m_1(x_t) = 0, \qquad (21)$$

which gives that

$$v_a(x_t) = \frac{\omega_r}{k}. \qquad (22)$$

This will remain a reasonable approximation to the point where the nature of the mode becomes dominantly evanescent for complex ω if $\omega_r/\omega_i \gg 1$, which will be the case for the waveguide modes that we will examine.

Since $k = \sqrt{k_y^2 + k_z^2} \geq k_z$, the turning point occurs for a lower value of the Alfvén speed than the resonant point, which in our model means that

$$x_t > x_R. \qquad (23)$$

In other words, the resonant point is deeper in the magnetosphere than the turning point is.

The strength of the resonant coupling depends on the distance between the turning point and the resonant point. The points may only coincide when $k = k_z$ (i.e., $k_y = 0$). However, the resonance occurs in the y component of the perturbed velocity, and since this is defined from the linearized ideal MHD equations as

$$u_y = \frac{k_y \omega}{\rho_1 (\omega^2 - k_z^2 v_a^2)} p_T, \qquad (24)$$

there will be no coupling when $k_y = 0$. As k_y increases from zero, the decay length in x of the fast mode ($\approx 1/m_1$) decreases, and the separation of x_t and x_R increases. Thus the amplitude of the fast mode becomes very small as k_y becomes large, and very little energy may penetrate to drive a resonance in this limit. Thus the strength of the resonant coupling first increases and then decreases with k_y as the resonant point moves away from the the turning point [Kivelson and Southwood, 1986].

3. Results

We will examine the behavior of the first three body mode harmonics when $k_z = \pi$, taking also the flow speed $v_o = 10$ and $\rho_1 (x = 1) = 0.192$ (which we will use for all our results). We have used a flow speed slightly higher than those commonly observed on the flanks of the magnetosphere in order to examine various unstable harmonics in both x and z. As shown by Mills et al. [1999] the onset of instability for fast cavity modes is given by

$$v_o = \frac{v_a + c_s}{\sin \alpha}, \qquad (25)$$

where $\alpha = \tan^{-1}(k_y/k_z)$ and is the angle between the vector $\mathbf{k}$ and the equilibrium magnetic field $\mathbf{B_1}$. Thus choosing a large value of the flow ensures that we can study several harmonics for larger values of k_z. In this section we will consider only modes having $k_z = \pi$; however, we will consider the phase speeds for other k_z, v_o and ϵ in section 5.
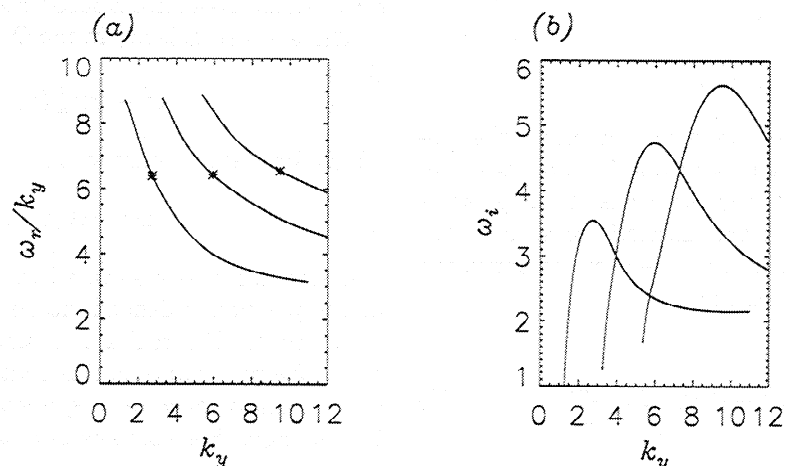

Figure 2. The first three harmonics in x when $k_z = \pi$, $v_R = 8$, and $v_o = 10$: (a) and growth rates (b). The asterisks show the phase speed at maximum growth rate for each of the modes.

Figure 2 shows the phase speeds and growth rates of the first three harmonics of the body modes when $k_z = \pi$ and $v_R = 8$. The maxima in the growth rates of the modes occur for $k_y = 2.73$, 5.93, and 9.48. The corresponding phase speeds at maximum growth rate are $\omega_r/k_y = 6.40$, 6.43, and 6.55, respectively, and these are shown by asterisks in Figure 2a. The modes most likely to be observed are those that have the largest growth rates, i.e., those for which the growth rate is a maxima. The phase speeds of these modes at the maxima are very similar, and this implies that the observed modes would have similar phase speeds: a prediction in excellent agreement with the observations reported by *Ziesolleck and McDiarmid* [1994].

Now we will look at the fastest growing part of these three modes in more detail. Figure 3a shows the eigenfunction u_{yr} (the real part of the perturbed velocity in the y-direction) as a function of x, and Figure 3b shows the Alfvén speed profile. In Figure 3a the dashed and dash-dotted lines indicate the positions of the turning and resonant points (x_t and x_R), respectively, and in Figure 3b show the corresponding values of the Alfvén speed. The wavenumber is dominantly imaginary when $x < x_t$, and it would be reasonable to expect the solution to appear evanescent in this region. However, we see a clearly defined waveform centered around the point x_R. This is an Alfvén resonance centered close to the predicted position of the singularity based on ω_r. Figure 4 shows the magnitude of $u_y(= \sqrt{u_{yr}^2 + u_{yi}^2})$ as a function of x. The strong peak here corresponds to the Alfvén resonance.

Figure 5 shows the eigenfunction and Alfvén speed profile for the fastest growing part of the second harmonic mode. Again, we see there is a clearly defined resonance near the predicted value of x_R. The resonant point is deeper inside the magnetosphere for this mode and is farther from the turning point.

Finally, Figure 6 shows the eigenfunction and speed profile for the fastest growing part of the third harmonic. Here k_y is much larger than it is for the fundamental mode, and the resonant point is much deeper in the magnetosphere. The coupling strength is also much less strong, and the resonance is much smaller compared to the background oscillation. However, in this case, because of the fact that this is a higher harmonic, we can more clearly see that the mode is dominantly oscillatory between the magnetopause and the turning point but that it becomes dominantly evanescent beyond that point.

For the values of flow speed v_o, Alfvén profile v_R and wavenumber k_z chosen, there are three resonances occurring within the magnetosphere, all having very similar values of phase speed. Now we examine the theory of wave overreflection at the magnetopause which enables us to understand the consistency of the phase speeds.

4. Theory of Wave Overreflection

A useful concept in understanding the unstable behavior of our modes is that of wave overreflection. We now consider a model with an unbounded uniform magnetosphere and consider the effect of a wave impinging on the magnetopause boundary from within the magnetosphere. We assume that some part of the wave is reflected back into the magnetosphere and that some part is transmitted through the magnetopause to propagate in the magnetosheath. Figure 7 gives a schematic view of these three waves.

Sen [1964], and later *Pu and Kivelson* [1983], showed that for a compressible plasma there are two important speeds in considering the development of the instability at a flow discontinuity between unbounded plasmas. *Southwood* [1968] also found these two speeds and showed that they could be predicted [see also *Mills et*
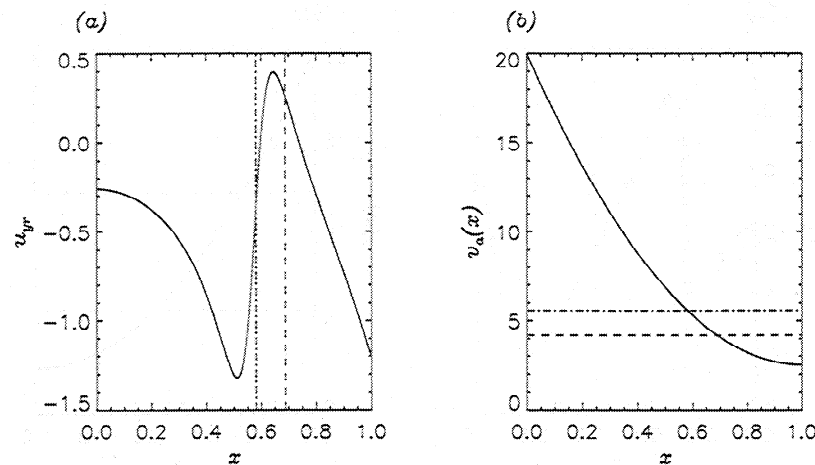

Figure 3. The fastest growing part of the fundamental mode (corresponding to $k_y = 2.73$, $v_p = 6.40$, and $\omega_i = 3.55$) when $v_o = 10$ and $v_R = 8$: (a) eigenfunction u_{yr} and (b) Alfvén speed profile. The vertical lines in Figure 3a show the positions of the turning point, x_t (dashed line), and the resonant point, x_R (dash-dotted line). The horizontal lines in Figure 3b show the corresponding values of $v_a(x)$ at those points.
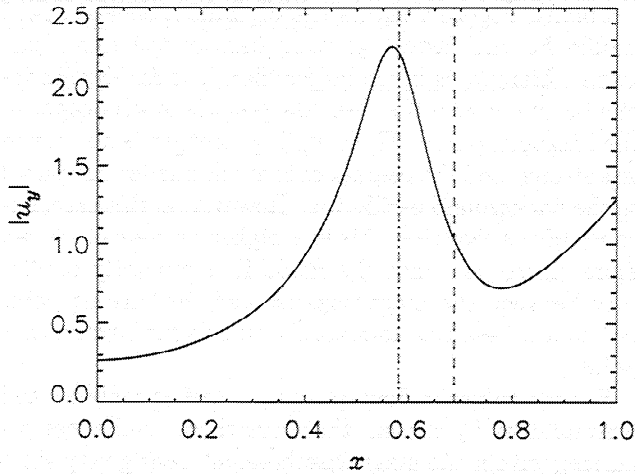
Figure 4. The magnitude of the complex function u_y as a function of x for the parameters shown in Figure 6. The vertical lines show the position of the turning point, x_t (dashed line), and the resonant point, x_R (dash-dotted line) predicted for stable modes.

al., 1999]. The first speed, v_c, is the minimum speed at which instability can occur; at a higher speed, v_u, stability is regained, and the modes become purely oscillatory on both sides of the discontinuity.

McKenzie [1970] showed that the reflection coefficient for this system (the ratio of the amplitude of the reflected wave to that of the incident wave) is given by

$$R = \frac{1-Z}{1+Z}, \tag{26}$$

where for our system,

$$Z = \frac{m_1 (\omega - k_y v_o)^2}{m_2 \epsilon (\omega^2 - k_z^2 v_{a1}^2)}, \tag{27}$$

where $\epsilon = \rho_1 / \rho_2$.

In deriving equations (26) and (27) we have assumed that ω is purely real and that m_1 is also real (so that we do actually have a wave propagating in the magnetosphere). The sign of m_1 is taken to be positive so that the group velocities of the incident and reflected waves are in the correct sense. Unlike the bounded case that we considered in section 2, stable modes may exist with $m_2^2 > 0$ (i.e, m_2 is real). In this case, the modes are purely evanescent on both sides of the magnetopause for low flow speeds. As the flow speed increases, the system becomes unstable, but if the flow speed is further increased, the mode restabilizes, becoming oscillatory on both sides of the magnetopause. According to equation (4) there are two possibilities for the sign of m_2^2: (i) $m_2^2 < 0$ and (ii) $m_2^2 > 0$.

In case 1, m_2 is purely imaginary, and thus Z is also purely imaginary ($Z = i|Z|$). Thus

$$R = \frac{1 - i|Z|}{1 + i|Z|}, \tag{28}$$

$$|R| = 1. \tag{29}$$

In this case, we have total internal reflection of magnetospheric waves, and there is no transmitted wave (we have an exponential decay into the magnetosheath).

Conversely, in case 2, Z is real, and therefore R is also real. We may now subdivide this case into two further possibilities: $Z < 0$ and $Z > 0$. If $Z < 0$, then $R > 1$, and we have overreflection In fact, $|R| \to \infty$ when $Z = -1$, implying that

$$m_1 (\omega - k_y v_o)^2 + m_2 \epsilon (\omega^2 - k_z^2 v_{a1}^2) = 0, \tag{30}$$

which is the dispersion relation for stable oscillatory modes for the unbounded magnetosphere model. Thus overreflection of modes may occur only when $m_2^2 > 0$, corresponding to the mode being oscillatory on both
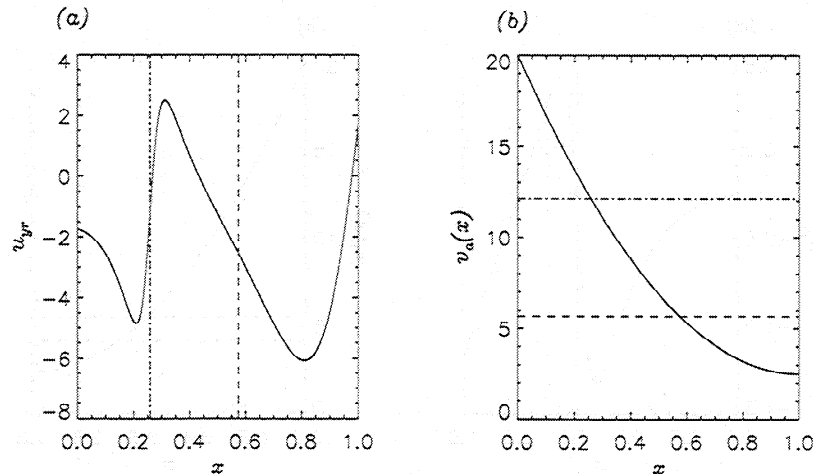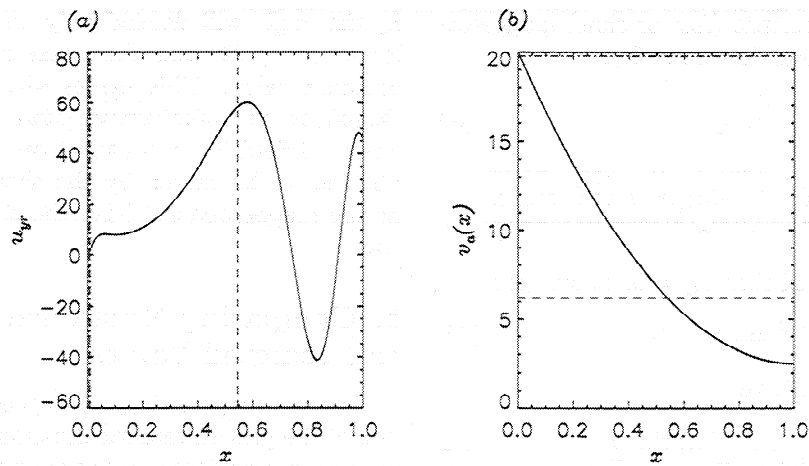

Figure 5. The fastest growing part of the second harmonic mode (corresponding to $k_y = 5.93$, $v_p = 6.43$, and $\omega_i = 4.74$) when $v_o = 10$ and $v_R = 8$: (a) eigenfunction u_{yr} and (b) Alfvén speed profile. The vertical lines in Figure 5a show the positions of the turning point, x_t, (dashed line), and the resonant point, x_R (dash-dotted line). The horizontal lines in Figure 5b show the corresponding values of $v_a(x)$ at those points.

Figure 6. The fastest growing part of the second harmonic mode (corresponding to $k_y = 9.48$, $v_p = 6.55$, and $\omega_i = 5.63$) when $v_o = 10$ and $v_R = 8$: (a) eigenfunction u_{yr} and (b) Alfvén speed profile. The vertical lines in Figure 6a show the positions of the turning point, x_t (dashed line), and the resonant point, x_R (dash-dotted line). The horizontal lines in Figure 6b show the corresponding values of $v_a(x)$ at those points.

sides of the magnetopause. In the bounded case, the modes do not restabilize but remain unstable for all flow speeds above the onset of instability, so we will compare the results found using these stable oscillatory modes to those found in our numerical model for unstable modes. Note that in the case of stable oscillatory modes on both sides of the interface, the phase speed must be below $v_o \sin \alpha - c_s$, and therefore $\omega - k_y v_o < 0$. Thus we must choose $m_2 < 0$ in order to satisfy equation (6). Hence [*McKenzie*, 1970, p.6] "a resonance is excited when the incident wave frequency matches the frequency of one of the characteristic frequencies of the vibrations of the interface". This is also the condition corresponding to waves being spontaneously radiated away from the boundary even as the amplitude of the incident wave vanishes. When $Z > 0$, $R < 1$, and we have the normal case of partial reflection. We will derive the particular conditions for overreflection in each case we examine.

Assuming that $m_2^2 > 0$, we may now define (following *McKenzie* [1970])

$$\mathbf{k}_1 = (m_1, k_y, k_z)$$
$$= k_1 (\cos \theta_1, \sin \theta_1 \sin \alpha, \sin \theta_1 \cos \alpha), \quad (31)$$

$$\mathbf{k}_2 = (m_2, k_y, k_z)$$
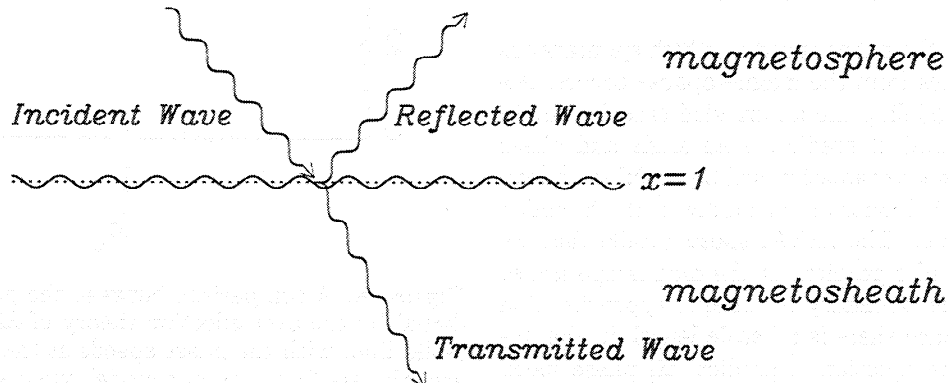$$= k_2 (\cos \theta_2, \sin \theta_2 \sin \alpha, \sin \theta_2 \cos \alpha), \quad (32)$$

where α is the angle between the vector $(0, k_y, k_z)$ and the equilibrium magnetic field $\mathbf{B}_1$, $\theta_{1,2} = \tan^{-1}(k/m_{1,2})$, and Snell's law requires that $k_1 \sin \theta_1 = k_2 \sin \theta_2$. Substituting these values into equation (27) and noting that

$$(\omega - k_y v_o)^2 = \omega'^2 = k_2^2 c_{s2}^2, \quad (33)$$

we obtain

$$Z = \frac{\sin 2\theta_1 c_{s2}^2}{\epsilon \sin 2\theta_2 \left(U^2 - v_{a1}^2 \sin^2 \theta_1 \cos^2 \alpha\right)}, \quad (34)$$

Figure 7. A schematic representation of the incident, reflected, and transmitted waves at the magnetopause.

where U is the characteristic (fast or slow) magnetoacoustic phase speed along the vector $\mathbf{k_1}$,

$$U^2 = \frac{\omega^2}{k_1^2} = \frac{v_{a1}^2 + c_{s1}^2}{2} \pm \frac{\sqrt{(v_{a1}^2 + c_{s1}^2)^2 - 4v_{a1}^2 c_{s1}^2 \sin^2\theta_1 \cos^2\alpha}}{2}. \quad (35)$$

In fact, we have assumed that $c_{s1} = 0$, so we have

$$U^2 = v_{a1}^2. \quad (36)$$

Noting that, using Snell's law,

$$m_2^2 = k_2^2 \cos^2\theta_2 = \frac{k_1^2 \sin^2\theta_1}{\tan^2\theta_2}, \quad (37)$$

we may define

$$\tan\theta_2 = \pm\frac{\sin\theta_1}{\lambda}, \quad (38)$$

where (using equations (4), (5), (31), and (35))

$$\lambda^2 = \frac{m_2^2}{k_1^2} = \frac{(U - v_o \sin\theta_1 \sin\alpha)^2 - c_{s2}^2 \sin^2\theta_1}{c_{s2}^2}. \quad (39)$$

Hence we may substitute for $\sin 2\theta_2$ in equation (34) using the identity

$$\sin 2\theta_2 = \pm\frac{2\lambda \sin\theta_1}{\lambda^2 + \sin^2\theta_1}. \quad (40)$$

Hence Z is now defined as

$$Z = \pm\frac{\cos\theta_1 (U - v_o \sin\theta_1 \sin\alpha)^2}{\epsilon\lambda (U^2 - v_{a1}^2 \sin^2\theta_1 \cos^2\alpha)}, \quad (41)$$

where the sign is again chosen to satisfy the outgoing group velocity condition in the magnetosheath (Z is chosen to have the same sign as that for the real part of m_2).

We may now solve the equation $Z = -1$ to find the value of the angle, θ_1, at which resonance (or spontaneous radiation of modes) may occur. Then using the fact that the azimuthal phase speed is

$$v_p = \frac{\omega}{k_y} = \frac{U}{\sin\theta_1 \sin\alpha}, \quad (42)$$

we may also find the phase speed at which spontaneous radiation of modes from the magnetopause occurs. Although this is modeling the unbounded case for purely real ω, this method of predicting an angle and phase speed for spontaneous radiation will be useful in analyzing the unstable behavior of our modes in the bounded nonuniform model. The Alfvén speed profile that we have chosen has zero gradient at the magnetopause, so that close to this boundary a uniform approximation is reasonable. Since there is no scale length in the unbounded case, the equation to predict this phase speed (equation (42)) is independent of k and depends only on the angle between the magnetic field and the propagation vector, α. Since $\alpha = \tan^{-1}(k_y/k_z)$, for a fixed

k_z the angle will depend only on k_y. As k_y becomes large, $\alpha \to \pi/2$, and the phase speed will tend to a constant value. This agrees with the observations of *Ziesolleck and McDiarmid* [1994] that simultaneously observed field line resonances on the flanks (which are believed to be driven by the shear flow discontinuity at the magnetopause) have the same azimuthal phase speed.

5. Comparing Numerical Results to Predicted Values

Now we compare the phase speeds found at the maxima of the growth rate for the modes found in section 3 with those predicted by the formula in section 4. Figure 8 shows the value of ω_r/k_y predicted by placing $Z = -1$ in equation (41) and evaluating equation (42) as a function of k_y (using $v_o = 10$ and $k_z = \pi$). The symbols represent the values found by the numerical model with $v_R = 8$ for the fundamental mode, second harmonic, and third harmonic. We can see that the numerical values fall very close to the predicted values, with the fit getting better for higher harmonics. The larger discrepancy seen for the fundamental mode may be explained by the fact that this mode has a wavelength approximately twice the width of our cavity, and so the approximation of an infinite, uniform magnetosphere does not compare well to this mode which has no real oscillations between the magnetopause and the turning point. Note that the predicted value of the phase speed is almost constant for $k_y > 3$, which agrees well with the fact that observed FLRs have constant phase speed.
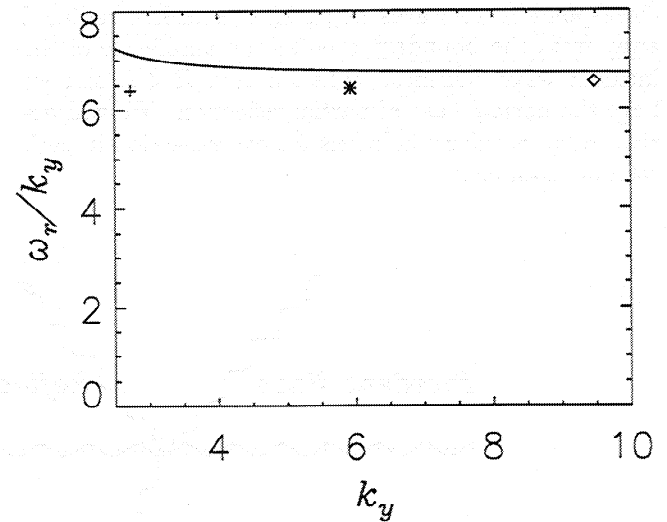

Figure 8. A comparison between the phase speed predicted by the overreflection theory of *McKenzie* [1970] (solid line) with the phase speeds at the maxima of the growth rate found by our model when $k_z = \pi$, $v_R = 8$, and $v_o = 10$ for the fundamental (cross), second harmonic (asterisk), and third harmonic (diamond) in the x direction.

Figure 9 shows the predicted value of the phase speed at the maximum growth rate as a function of α with the actual values for the second, third, and fourth harmonics. The values of k_z for those harmonics are (from right to left) $\pi/2$, π, $3\pi/2$, 2π, and $5\pi/2$. The variation of the predicted phase speed for these angles is relatively small, again corresponding well to observed modes having a consistent phase speed. The agreement between the predictions and the results found by our model is excellent, with best agreement occurring for higher harmonics in both x and z.

Finally, we compare the numerical and analytical results for the different harmonics in x and several values of v_R when $k_z = \pi/2$. Figure 10 shows the predicted value of the phase speed with the values found at maximum growth rate in our model for the first, second, and third harmonics. The values of v_R increase from left to right. Once again, the agreement is excellent, with the higher modes agreeing more closely. The agreement is best for low values of v_R (which corresponds most closely to a uniform magnetosphere) but is good for all values. Thus the phase speeds predicted by the infinite uniform magnetosphere model may be used as a reasonable estimate of the phase speeds we expect to observe in the magnetosphere.

We saw in Figures 9 and 10 that the value of the phase speed at which we expect spontaneous radiation of modes varies little with k_y or α. The values of the phase speed at maximum growth rate found in our model are also remarkably insensitive to the variation of the Alfvén speed in the magnetosphere. In fact, if we take the limit $k_y/k_z \gg 1$, then $\alpha \approx \pi/2$, and this provides a simple limit in which to evaluate the approx-
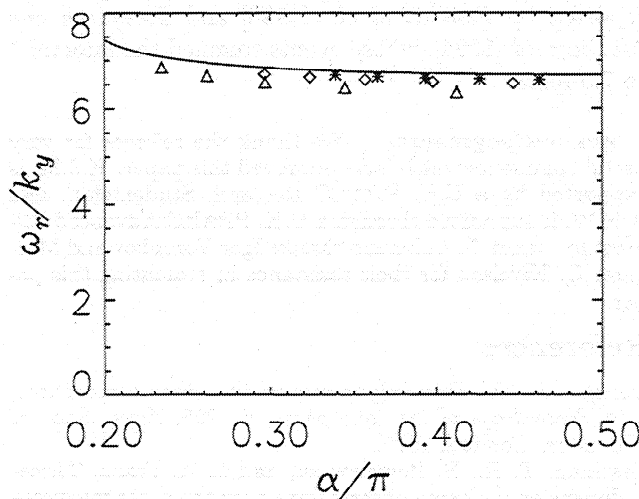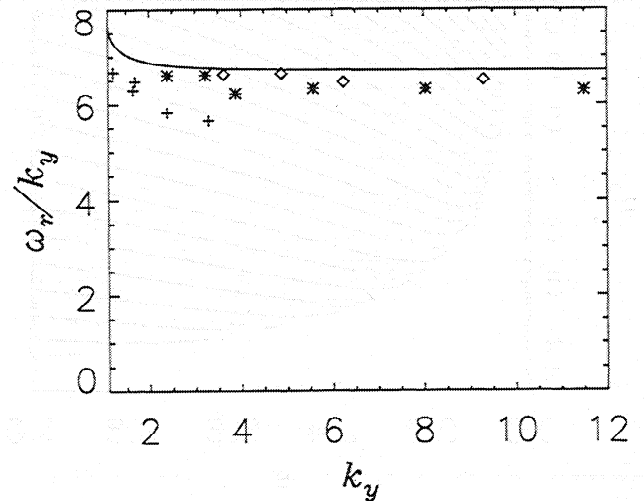

Figure 10. The predicted phase speed at maximum growth rate and the values found by our model for the first (crosses), second (asterisks), and third (diamonds) radial harmonics for various values of v_R (from left to right, $v_R = 1$, 2, 4, 8, and 16) when $v_o = 10$ and $k_z = \pi/2$.

imately constant phase speed. (We do not suggest that k_y/k_z is large for real ULF waves, since this would provide very weak coupling between fast and Alfvén waves, Rather, we note that as the phase speed is insensitive to k_y, this limit is adopted merely for ease of calculation of the phase speed.) Thus we may now calculate the phase speed for spontaneous radiation of waves from the magnetopause when $\alpha = \pi/2$ and use this to predict the values of the phase speeds of field line resonances in the magnetosphere. We also assume that $\gamma = 2$ for this calculation so that the fast speed U may be simplified such that

$$U = v_{a1} = \frac{c_{s2}}{\sqrt{\epsilon}}, \tag{43}$$

where $\epsilon = \rho_1(1)/\rho_2$. Using these approximations, we find that

$$Z = \pm \frac{\cos\theta_1 \left(c_{s2}/\sqrt{\epsilon} - v_o \sin\theta_1\right)^2}{\lambda c_{s2}^2}$$

$$= \pm \frac{\cos\theta_1 \left(\epsilon^{-1/2} - v_o \sin\theta_1\right)^2}{\left[\left(\epsilon^{-1/2} - v_o \sin\theta_1\right)^2 - \sin^2\theta_1\right]}, \tag{44}$$

where we have used the fact that $c_{s2} = 1$ since we have normalized our variables. Solving, for θ_1, we can then find the phase speed,

$$v_p = \frac{1}{\sqrt{\epsilon}\sin\theta_1}. \tag{45}$$

Figure 9. The predicted phase speed at maximum growth rate and the values found by our model for the second (triangles), third (diamonds), and fourth (asterisks) harmonics for various values of k_z (from left to right for each harmonic, the values of k_z are $5\pi/2$, 2π, $3\pi/2$, π, and $\pi/2$) when $v_o = 10$. Here we have used $v_o = 10$ and $v_R = 8$.

Figure 11 shows the values of the phase speed as a contour plot as a function of v_o (the sonic Mach number of the flow in the magnetosheath) and the ratio of the density in the magnetosphere to that in the magnetosheath, ϵ. Spontaneous radiation of modes may
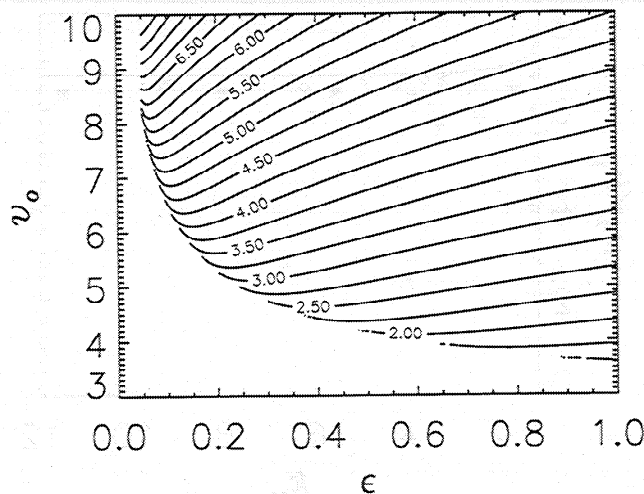
Figure 11. The predicted phase speed (normalized to the magnetosheath sound speed) at maximum growth rate as a function of the ratio of densities in the magnetosphere and magnetosheath, $\epsilon = \rho_1/\rho_2$, and the sonic Mach number in the magnetosheath, v_o.

only occur above the upper critical speed (at which the modes stabilize in the unbounded uniform case), and thus we may only predict a phase speed for relatively high flow speeds. We can see that for a given density ratio the phase speed at spontaneous radiation increases for increasing flow speed. However, increasing the ratio of densities, ϵ decreases the predicted phase speed. Although the phase speeds in Figure 11 are approximate, they provide very reliable estimates. For example, the parameters used in Figure 10 ($\epsilon = 0.192$, and $v_o = 10$) may be used in conjunction with Figure 11 to infer a phase speed of 6.7, which is in good agreement with the true values.

Observations show that the density ratio (and therefore the ratio of the Alfvén speed in the magnetosphere to the sound speed in the magnetosheath) across the magnetopause varies greatly for different magnetopause crossings. *Eastman et al.* [1985] found Alfvén speeds in the magnetosphere ranging from 200 to 1500 km/s. Typical magnetosheath sound speeds are in the range 100 to 150 km/s (see observations discussed by *McKenzie*, [1970]). The ratio of the Alfvén speed at the magnetopause, $v_a(1)$, to the sound speed in the magnetosheath, c_s, can be related to the density ratio, ϵ, using

$$\frac{v_a(1)}{c_s} = \sqrt{\frac{5}{6\epsilon}}. \qquad (46)$$

Using Figure 11, our predictions may be compared to observational results if either the ratio of the densities or of the speeds is measured. For the values quoted above, ϵ lies in the range 0.005 to 0.5.

6. Conclusions

We have presented a model for the excitation of Alfvén resonances in the magnetosphere by fast cavity modes driven by the shear flow discontinuity at the magnetopause. We calculated the expected phase speed at maximum growth rate following *McKenzie* [1970] and showed that the total variation of this speed over the unstable cavity modes was of the order of 10%. We compared our results to this prediction and showed that our results agree well with the predictions, with accuracy increasing for higher harmonics in both x and z. We would expect observed phase speeds to be close to the predictions and, for any given flow speed, to be similar for all simultaneously excited resonances. This is in excellent agreement with the work of *Ziesolleck and McDiarmid* [1994].

Taking the sound speed in the magnetosphere to be about 100 km/s, the depth of the magnetosphere to which modes will penetrate to be of the order of 10 R_E, and the plasma density in the magnetosheath to be 5 times that in the magnetosphere, we may compare the values predicted by our model with those observed in the magnetosphere. For a flow speed of about 600 km/s the phase speed we predict is about 400 km/s. Observations using HF radar report simultaneously observed Pc5s having phase speeds of between 50 and 250 km/s (see Table 1 of *Fenrich et al.*, [1995]). Magnetometer data show Pc5 oscillations having phase speeds of between 500 and 1000 km/s [*Ziesolleck and McDiarmid*, 1994], which is somewhat higher than those observed by radar. Our predicted phase speed lies between these observed values. At this flow speed the fundamental body mode for $v_R = 1$ has $\omega_r \approx 10$, which corresponds to a period of oscillation of about 400 s or a frequency of the order of 2.5 mHz. This frequency is typical of those reported by *Fenrich et al.* [1995] and *Ziesolleck and McDiarmid* [1994], whose events spanned the interval 1 to 7.5 mHz.

References

Dungey, J. W., Electrodynamics of the outer atmosphere, in *Proceedings of the Ionosphere*, p. 255, Phys. Soc. of London, London, 1955.

Eastman, T. E., B. Popielawska, and L. A. Frank, Three-dimensional plasma observations near the outer magnetospheric boundary, *J. Geophys. Res., 90*, 9519, 1985.

Engebretson, M., K.-H. Glassmeier, M. Stellmacher, W. J. Hughes, and H. Lühr, The dependence of high-latitude Pc5 wave power on solar wind velocity and on the phase of high-speed solar wind streams, *J. Geophys. Res., 103*, 26,271, 1998.

Fenrich, F. R., J. C. Samson, G. Sofko, and R. A. Greenwald, ULF high- and low-*m* field line resonances observed with the Super Dual Auroral Radar Network, *J. Geophys. Res.*, *100*, 21,535, 1995.

Fujita, S., K.-H. Glassmeier, and K. Kamide, MHD waves generated by the Kelvin-Helmholtz instability in a nonuniform magnetosphere, *J. Geophys. Res.*, *101*, 27,317, 1996.

Hughes, W. J., Magnetospheric ULF waves: A tutorial with a historical perspective, in *Solar Wind Sources of Magnetospheric Ultra-Low-Frequency Waves, Geophys. Monogr. Ser.*, vol 81, edited by M. J. Engebretson, K. Takahashi, and M. Scholer, p. 1-12, AGU, Washington, D.C., 1994.

Kivelson, M. G., and D. J. Southwood, Resonant ULF waves: A new interpretation, *Geophys. Res. Lett.*, *12*, 49, 1985.

Kivelson, M. G., and D. J. Southwood, Coupling of global magnetospheric MHD eigenmodes to field line resonances, *J. Geophys. Res.*, *91*, 4345, 1986.

Mann, I. R., A. N. Wright, K. J. Mills, and V. M. Nakariakov, Excitation of magnetospheric waveguide modes by the magnetosheath flow, *J. Geophys. Res.*, *104*, 333, 1999.

McKenzie, J. F., Hydromagnetic wave interaction with the magnetopause and the bow shock, *Planet. Space Sci.*, *18*, 1, 1970.

Miles, J. W., On the reflection of sound at an interface of relative motion, *J. Acoust. Soc. Am.*, *29*, 226, 1957.

Mills, K. J., A. N. Wright, and I. R. Mann, Kelvin-Helmholtz driven modes of the magnetosphere, *Phys. of Plasmas*, in press, 1999.

Pu, Z. Y., and M. G. Kivelson, Kelvin-Helmholtz instability at the magnetopause: Solution for compressible plasmas, *J. Geophys. Res.*, *88*, 841, 1983.

Ribner, H. S., Reflection, transmission, and amplification of sound by a moving medium, *J. Acoust. Soc. Am.*, *29*, 435, 1957.

Rickard, G. J., and A. N. Wright, Alfvén resonance excitation and fast wave propagation in magnetospheric waveguides, *J. Geophys. Res.*, *99*, 13,455, 1994.

Rickard, G. J., and A. N. Wright, ULF pulsations in a magnetospheric waveguide: Comparison of real and simulated satellite data, *J. Geophys. Res.*, *100*, 3531, 1995.

Sen, A. K., Effect of compressibility on Kelvin-Helmholtz instability in a plasma, *Phys. Fluids*, *7*, 1293, 1964.

Southwood, D. J., The hydromagnetic stability of the magnetospheric boundary, *Planet. Space Sci.*, *16*, 587, 1968.

Southwood, D. J., Some features of field-line resonances in the magnetosphere, *Planet. Space Sci.*, *22*, 483, 1974.

Walker, A. D. M., Excitation of magnetohydrodynamic cavities in the magnetosphere, *J. Atmos. Sol. Terr. Phys.*, *60*, 1279, 1998.

Walker, A. D. M., J. M. Ruohoniemi, K. B. Baker, and R. A. Greenwald, Spatial and temporal behavior of ULF pulsations observed by the Goose Bay HF radar, *J. Geophys. Res.*, *97*, 12,187, 1992.

Wright, A. N., Dispersion and wave coupling in inhomogeneous MHD waveguides, *J. Geophys. Res.*, *99*, 159, 1994.

Wright, A. N., and G. J. Rickard, ULF pulsations driven by magnetopause motions: Azimuthal phase characteristics, *J. Geophys. Res.*, *100*, 23,703, 1995.

Zhu, X. M., and M. G. Kivelson, Analytic formulation and quantitative solutions of the coupled ULF wave problem, *J. Geophys. Res.*, *93*, 8602, 1988.

Ziesolleck, C. W. S., and D. R. McDiarmid, Auroral latitude Pc5 field line resonances: Quantized frequencies, spatial characteristics, and diurnal variations, *J. Geophys. Res.*, *99*, 5817, 1994.

K. J. Mills and A. N. Wright, Mathematical Institute, University of St. Andrews, St. Andrews, Fife KY16 9SS, Scotland, U.K. (katie@dcs.st-and.ac.uk; andy@dcs.st-and.ac.uk)